

## ALLANITE-(Ce) FROM THE EOCENE CASTO GRANITE, IDAHO: RESPONSE TO HYDROTHERMAL ALTERATION

SCOTT A. WOOD<sup>§</sup> AND ALICE RICKETTS

Department of Geological Sciences, University of Idaho, Box 443022, Moscow, Idaho 83844-3022, U.S.A.

### ABSTRACT

The response of allanite-(Ce) in the Eocene Casto granite of Idaho to hydrothermal activity has been investigated. Unaltered, igneous allanite from the Casto pluton is characterized by a narrow range of compositional variation, with little or no zoning. A representative empirical formula, based on the composition of the least-altered grain, is:  $(REE_{0.83}Ca_{1.07}Th_{0.04}Mn^{2+}_{0.06})(Ti^{4+}_{0.11}Mg^{2+}_{0.04}Fe^{2+}_{0.99}Fe^{3+}_{0.48}Al_{1.38})(Si_{3.00}O_{12})(OH_{0.95}F_{0.05})$ , where *REE* represents  $(La_{0.14}Ce_{0.41}Pr_{0.05}Nd_{0.17}Sm_{0.03}Y_{0.03})$ . The small amount of observed compositional variation is consistent with the coupled substitutions  $Ca^{2+} + Th^{4+} \leftrightarrow 2REE^{3+}$  and  $REE^{3+} + Fe^{2+} + Mg^{2+} \leftrightarrow Ca^{2+} + Al^{3+} + Fe^{3+}$ . Slightly altered crystals exhibit a rim in which Th is enriched, and La and Ce are depleted. Increasing alteration lead to extensive corrosion and replacement of allanite by fluorite, a *REE*-, Th- and P-rich phase (probably monazite), and a Th-rich phase (probably thorianite). In spite of attack by fluoride-rich hydrothermal solutions, the *REE* and Th originally in allanite were not transported significant distances, but were redeposited locally as secondary phases. The lack of significant *REE* and Th transport is due to the availability of phosphorus, which allowed the *REE* to be fixed in a secondary phosphate phase, and the removal of fluoride as fluorite. This work has implications for the behavior of radioactive waste in deeply buried geological repositories upon interaction with heated groundwaters.

**Keywords:** allanite-(Ce), monazite-(Ce), hydrothermal alteration, radioactive waste analogue, rare- earth elements, thorium, Casto granite, Idaho.

### SOMMAIRE

Nous avons étudié le comportement de l'allanite-(Ce) dans le granite éocène de Casto, en Idaho, en présence d'une activité hydrothermale. L'allanite saine et primaire démontre un intervalle de composition très restreint, et très peu d'évidence de zonation. Une composition représentative des cristaux les moins affectés serait  $(TR_{0.83}Ca_{1.07}Th_{0.04}Mn^{2+}_{0.06})(Ti^{4+}_{0.11}Mg^{2+}_{0.04}Fe^{2+}_{0.99}Fe^{3+}_{0.48}Al_{1.38})(Si_{3.00}O_{12})(OH_{0.95}F_{0.05})$ , dans laquelle *TR* (terres rares) représente  $(La_{0.14}Ce_{0.41}Pr_{0.05}Nd_{0.17}Sm_{0.03}Y_{0.03})$ . La faible variation en composition résulte des substitutions couplées  $Ca^{2+} + Th^{4+} \leftrightarrow 2TR^{3+}$  and  $TR^{3+} + Fe^{2+} + Mg^{2+} \leftrightarrow Ca^{2+} + Al^{3+} + Fe^{3+}$ . Les cristaux faiblement altérés font preuve d'un liseré dans lequel le Th est enrichi, et le La et le Ce sont appauvris. A mesure que le degré d'altération augmente, il y a corrosion importante et remplacement de l'allanite par la fluorite, un phosphate de *TR*, Th et P (probablement monazite), et un minéral riche en Th (probablement thorianite). Malgré l'attaque par des solutions riches en fluorures, les terres rares et le thorium originellement dans l'allanite n'ont pas été transportés très loin, mais plutôt redéposés localement sous forme de phases secondaires. Le transfert très limité des terres rares et du thorium serait attribuable à la disponibilité du phosphore, ce qui a permis aux terres rares d'être fixées dans un phosphate secondaire, avec l'élimination des fluorures sous forme de fluorite. Ce travail aurait des implications dans l'étude du comportement des éléments radioactifs lors de l'interaction de déchets radioactifs enfouis avec l'eau souterraine chauffée.

(Traduit par la Rédaction)

**Mots-clés:** allanite-(Ce), monazite-(Ce), altération hydrothermale, analogue de déchets radioactifs, terres rares, thorium, granite de Casto, Idaho.

### INTRODUCTION

The chemical and mineralogical response of natural allanite to hydrothermal alteration and the subsequent behavior of the *REE* (rare-earth elements) and Th (a common minor substituent in allanite) are relevant to

the prediction of the long-term behavior of deeply buried radioactive waste. Some nuclear waste ceramics such as SYNROC may contain allanite-like phases (Brookins 1984), and potentially metamict minerals such as allanite also may be useful proxies for borosilicate glass (Ewing 1976). Furthermore, the trivalent *REE*

<sup>§</sup> E-mail address: swood@iron.mines.uidaho.edu

and  $\text{Th}^{4+}$  are reasonable geochemical analogues of the trivalent actinides (*e.g.*,  $\text{Am}^{3+}$ ,  $\text{Cm}^{3+}$ ,  $\text{Bk}^{3+}$ ,  $\text{Pu}^{3+}$ ) and the tetravalent actinides (*e.g.*,  $\text{Pu}^{4+}$ ), respectively (*cf.* Choppin 1983, 1986, 1989, Brookins 1984, Millero 1992), which are not present in significant quantities in natural geological environments.

Two varieties of allanite are known to exist: allanite-(Ce), represented by  $(\text{Ce,Ca,Y})_2(\text{Al,Fe}^{2+},\text{Fe}^{3+})_3(\text{SiO}_4)_3(\text{OH})$ , and allanite-(Y), represented by  $(\text{Y,Ca,Ce})_2(\text{Al,Fe}^{2+},\text{Fe}^{3+})_3(\text{SiO}_4)_3(\text{OH})$ . This paper focuses on the former. Reports in the literature indicate that the breakdown of allanite-(Ce), owing to metamictization, hydrothermal alteration, and weathering, results in a variety of alteration products that tend to immobilize the REE and  $\text{Th}^{4+}$  in more stable secondary phases. Which secondary minerals develop depends on the physicochemical conditions of the fluid present (*i.e.*, pH, temperature, anion concentrations, *etc.*). The most commonly reported REE-bearing products of alteration are the REE fluorocarbonates, in particular bastnäsite,  $(\text{Ce,L a})\text{CO}_3\text{F}$ , and, to a lesser extent, synchysite,  $\text{Ca}(\text{Ce,L a})(\text{CO}_3)_2\text{F}$  (see Discussion for references). Other reported products of alteration include: unspecified phases or amorphous material (*e.g.*, Morin 1977), cerianite,  $\text{CeO}_2$  (Meintzer & Mitchell 1988), epidote (Carcangiu *et al.* 1997), lanthanite,  $(\text{La,Ce})_2(\text{CO}_3)_3 \cdot 8\text{H}_2\text{O}$  (Sæbø 1961), and monazite,  $(\text{Ce,L a})\text{PO}_4$  (see Discussion for references). The formation of monazite is of particular interest because it generally has been considered to be very stable

under natural geological conditions over long periods of time and has been considered as an alternative to borosilicate glass for actinide containment in the disposal of high-level nuclear waste (Boatner *et al.* 1980).

The Casto granitic pluton of central Idaho (Fig. 1), of Eocene age, contains abundant crystals of allanite, and there is good evidence for hydrothermal alteration in some parts of the pluton (see geological description below). Furthermore, the fluid phase responsible may have been relatively fluorine-rich, as indicated by the occurrence of fluorite veins in the altered granite. Fluoride is known to complex the REE and Th strongly (Wood 1990, Langmuir & Herman 1980), so the mobility of these elements should be higher in fluoride-rich than in fluoride-poor solutions. We have therefore undertaken a petrographic, SEM and electron-microprobe study to: 1) determine whether the allanite in the Casto pluton has been affected by this hydrothermal alteration, 2) document the mineralogical response, and 3) determine whether the REE and Th have been removed from the system or retained in secondary phases. We show that, in spite of the presence of fluoride, allanite is replaced by a phosphate phase in these rocks, and not bastnäsite. Furthermore, there appears to have been relatively little long-range mobility of the REE and Th. Upon their release from allanite during alteration, these elements have been immobilized by the formation of secondary phases in the immediate vicinity of the original allanite.

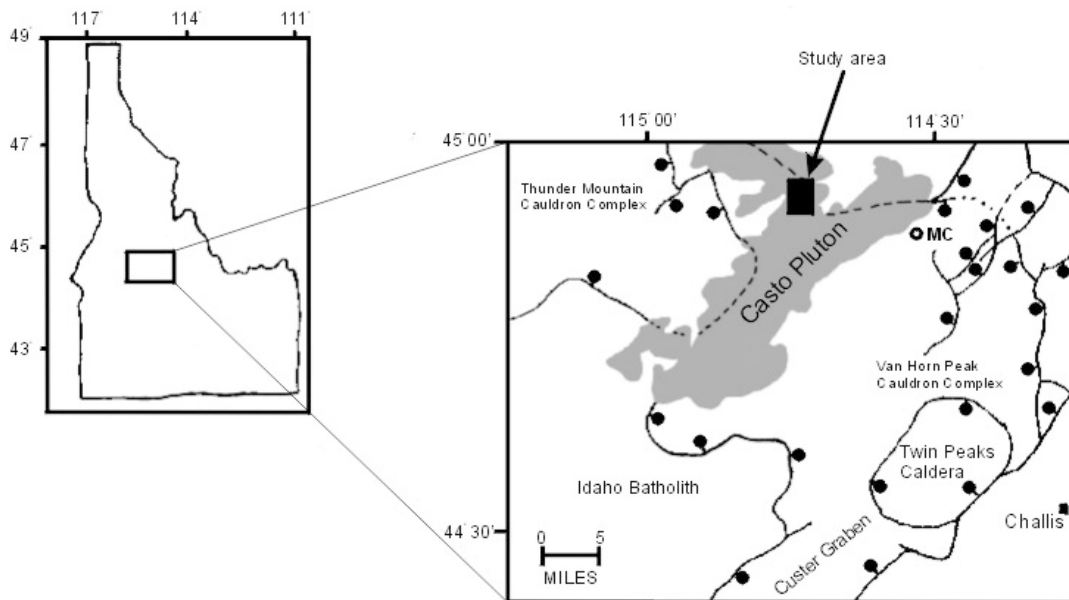


FIG. 1. Map showing location and geological setting of the Casto pluton. Black rectangle shows approximate location of the study area. Modified from Criss *et al.* (1984). MC indicates the location of the Meyers Cove fluorite deposits.

## GEOLOGICAL SETTING

The Casto pluton is located in the Salmon National Forest in central Idaho, along the Middle Fork of the Salmon River; most of the pluton lies in the north-central part of the Challis  $1^{\circ} \times 2^{\circ}$  quadrangle (Fig. 1). Samples were collected from Aparejo Point, north of BM 3755 at Aparejo Creek and north of Sheep Creek, 800 meters south of the Mormon Ranch (Aparejo Point  $7\frac{1}{2}$  minute quadrangle N4452.5–W11437.5). Samples were collected from this location because the rocks both contain abundant grains of allanite and seem to be among the most altered of any exposed rocks in the pluton.

The Casto granite is one of many Eocene plutons emplaced along the margin of the Idaho Batholith (Bennett 1980). The intrusion of the Idaho batholith occurred between 112 and 70 m.y. and dominated geological activity in the Cretaceous. Before and during the intrusion of the batholith, folding and eastward thrusting of Paleozoic sedimentary rocks took place. This folding and thrusting culminated during the Late Cretaceous Sevier orogeny, at which time the area was also subjected to some normal faulting and locally intense contact metamorphism. Igneous activity in the Tertiary included deposition of the Eocene Challis Volcanic Group, development of the Challis volcanic field, and intrusion of several batholiths and stocks. However, prior to this activity, the Idaho batholith was eroded, resulting in the local deposition of arkosic sediments. Volcanism was initiated about 51 m.y. ago with the widespread eruption of lavas of intermediate composition, and continued intermediately for another 5–6 m.y. The character of volcanism changed about 48 m.y. ago to predominantly ash-flow eruption, which led to the formation of the Van Horn Peak cauldron complex, the Custer Graben, and the Thunder Mountain and Twin Peaks calderas. Ages for the Casto intrusion obtained via the K–Ar method range from 46 to 43 Ma (Lewis & Kilsgaard 1991, Bennett & Knowles 1983, Fisher *et al.* 1992). Rocks in the Challis quadrangle have been affected by four major structural features. The northeast-trending Trans-Challis fault system is comprised of high-angle faults, fracture systems, dike swarms, and grabens. In addition, there is a north- and northwest-striking system of high-angle faults, caldera and collapse structures related to the Challis volcanic field, and several thrust faults in the Paleozoic rocks. These structures, particularly the Trans-Challis fault system, most likely provided conduits for the hydrothermal system that affected the Casto pluton. For more details on the regional tectonic and geological setting of the Casto pluton, consult Fisher & Johnson (1995), from which much of the above description was obtained.

Plutonic rocks of Eocene age in the Challis region are bimodal in character, and have been subdivided into a pink granite suite, comprising varieties of biotite granite, and a quartz monzodiorite suite, comprising

hornblende–biotite granite, granodiorite, quartz monzodiorite, diorite and gabbro (Lewis & Kilsgaard 1991). In general, granites in the area vary from fine- to coarse-grained, and are usually of characteristic pink color, although they may also be medium gray. Fisher *et al.* (1992) reported the modal composition of the Casto pluton to be in the range 22–34% quartz, 31–57% alkali feldspar (perthitic orthoclase and microcline), 18–33% plagioclase, 20–37% biotite, and 0–3.5% hornblende. Accessory minerals include zircon, magnetite, allanite, titanite and apatite. Fisher *et al.* (1992) noted that the composition of these rocks plots in the granite field delineated by Streckeisen (1973). The Casto and related plutons are considered to be anorogenic and related to intracontinental rifting or extension (Fisher & Johnson 1995).

Miarolitic cavities are common in the pink granites, including the Casto pluton, indicating that they were emplaced within a few kilometers of the surface and had reached saturation with respect to H<sub>2</sub>O (Bennett 1980, Bennett & Knowles 1983, Lewis & Kilsgaard 1991). The radioactivity of the Casto pluton is higher than that of the Idaho batholith rocks it intruded (Bennett 1980). The average radioactivity for the Idaho Batholith is reported to be 4000–5000 counts/second. Values for the Casto pluton, although not as high as in other Eocene plutons, are approximately double those of the Idaho batholith (Bennett 1980), and are much higher than average for granites.

Of particular relevance to this study are oxygen isotope studies, conducted by Criss *et al.* (1984) and Larson & Geist (1995), of the rocks of the pluton and surrounding areas. Rocks of the pre-existing Thunder Mountain Caldera are strongly altered, indicating that a large fossil hydrothermal system surrounded the Casto pluton. The Casto pluton has low and variable magmatic  $\delta^{18}\text{O}$  values, reflecting extensive assimilation of hydrothermally altered rocks at the level of emplacement (Larson & Geist 1995). In addition, Criss *et al.* (1984) showed that a circular pattern of isotopic disturbance centered on the Casto pluton occurs in the rocks surrounding the Casto pluton. These oxygen isotopic data suggest that the Casto pluton may have been subjected to alteration by hydrothermal fluids of meteoric origin. Fluorite vein-type deposits (Constantopoulos 1988) in the general area provide additional evidence of hydrothermal activity. Fluorite and chlorite veins were observed in the immediate study area, and as noted below, biotite, feldspar and allanite all record evidence of varying degrees of alteration in thin section. The Challis quadrangle is also well endowed with a variety of hydrothermal base- and precious-metal mineralization (Fisher & Johnson 1995). Hydrothermal activity continues to the present day in the general area, as evidenced by the existence of numerous hot springs along the margins of the Idaho Batholith (van Middlesworth & Wood 1998, and references therein).

## ANALYTICAL METHODS

A total of 35 granite samples were collected for this study, from which fifty polished thin sections were prepared. These thin sections were examined petrographically, and five were selected for further study. From these five thin sections, nine representative grains of allanite were chosen for analysis. On the basis of appearance under the petrographic microscope, the most altered is allanite grain 12A, the least altered is allanite grain 13A, and the others exhibit intermediate degrees of alteration.

First, quantitative analyses of allanite grains were obtained using a Cameca SX-50/PDP electron microprobe at the Department of Geological Sciences, University of Oregon (UO). The microprobe is equipped with four wavelength-dispersion spectrometers (WDS) and an energy-dispersion (EDS) attachment. We used pure  $\text{TiO}_2$  and a series of reference minerals as standards for major elements. Drake & Weill (1972) glass standards were used for the *REE*. The chemical composition of the standards is given in Appendix 1 of Ricketts (1994).

The allanite grains were analyzed for major elements at a voltage of 15 keV and a beam current of 10 nA for 10 seconds. Concentrations of the *REE* were established at 25 keV, with a beam current of 50 nA. Count time was 50 seconds for  $\alpha$ -lines, and 70 seconds for  $\beta$ -lines. To minimize peak interference, Ce, La, and Y readings were based on  $L\alpha$ -line emissions, Pr, Nd, and Sm readings were collected on  $L\beta$ , and Th on  $M\alpha$ -line emissions (Roedder 1985, Exley 1980). All others were collected on  $K\alpha$ -lines. The take-off angle was set at  $40^\circ$ .

In order to assess the spatial distribution of elements within the allanite grains and to identify possible products of alteration, back-scattered-electron images and X-ray maps of Si, Ca, Y, Th, Ce, La, P, and F distributions were prepared using the energy-dispersion (EDS) attachment of the electron microprobe. Element lines and instrument settings used were the same as those used for the quantitative analyses. Next, EDS scans of several areas within altered allanite grains were produced to provide qualitative elemental analysis of the alteration products.

Finally, whole-rock samples were analyzed for selected *REE* (La, Ce, Nd, Sm, Eu, Tb, Yb, Lu) by neutron activation at the Oregon State University Radiation Center. The accuracy of the analytical results was monitored by determination of *REE* concentrations in a series of reference materials (SRM 1633a, SRM 688, SRM 278, GSP-1 and CRB IV). In general, the results for these standard materials were within 5–10% of the accepted values.

## RESULTS

*Petrography*

In hand samples of the Casto granite, grain size varies over a scale of meters from fine (sugary in texture)

to coarse, and color ranges from gray to pink. The abundant minerals are quartz, orthoclase, plagioclase, and biotite. Amphibole is present in only a few samples, and in smaller proportions than biotite (1:2 or less). Additional minerals identifiable in the field were allanite, purple or green fluorite (in veins), and chlorite.

In thin section, quartz abundance ranges from 22 to 29 modal %, with an average of 24%. Quartz grains are euhedral to subhedral, usually colorless or smoky, and up to 3 mm in length. Most grains are fractured, and many show undulatory extinction. Orthoclase grains (21 to 36 modal %, 28% on average) are mostly subhedral, but some are anhedral, and up to 2.5 mm in length. Many samples display a granophyric texture. A perthitic texture also was identified in some samples. Plagioclase grains (18 to 22 modal %, 20% on average) vary in size from 1 to 15 mm. K-feldspar and plagioclase grains show varying degrees of conversion to white mica.

Biotite (5 to 12 modal %, 9% on average) is mostly subhedral to anhedral, ragged and chloritized. Some grains contain microscopic inclusions that could not be identified. Grain size varies up to 15 mm in length. Trace amounts (less than 0.1 modal %) of subhedral muscovite also were identified. The fluorine content of biotite is relevant in that fluoride is a strong complexer of the *REE* (Wood 1990) and could potentially be involved in *REE* remobilization. In the present study, the chemical composition of phases other than allanite was not established in detail. However, McIntyre *et al.* (1982) determined F content in biotite in other Tertiary granitic bodies in central Idaho to range between 1.2 and 4.2%.

Chlorite (4 to 8 modal %, 6% on average) occurs as an alteration product of biotite, in proximity to iron oxides. Chlorite grains are anhedral and less than 2 mm across. Allanite (0.4 to 4.1 modal %, 2.2% on average) is usually closely associated with biotite and chlorite, and occurs as euhedral to subhedral crystals. Grain size ranges from 1 to 15 mm. The physical appearance of allanite grains varies from fresh to highly altered (see below). Some grains show twinning, and others exhibit optical zonation. All appear to be metamict to varying degrees, as indicated by the presence of anastomosing cracks (Klein & Hurlbut 1985).

Apatite occurs as small (<0.1 mm), thin, euhedral prismatic crystals with a pale blue-green tint. It also occurs as inclusions in allanite as slightly larger, subhedral, tabular grains. Fluorite occurs mostly along fractures or in veins as granular masses or microscopic patches. It also occurs in miarolitic cavities. Zircon (< 1 vol.%) is seen as euhedral to subhedral inclusions in allanite or the other mafic minerals. Grain size is less than 0.5 mm. An opaque iron oxide (0 to 7 modal %, 2% on average) was tentatively identified as magnetite; ilmenite was not observed. Calcite occurs in small patches, usually together with fluorite. Titanite occurs as colorless to pale yellow, euhedral, wedge-shaped crystals, less than 2 mm in length.

## Electron-microprobe results

Representative results of quantitative electron-microprobe analyses are presented in Table 1 (additional results are tabulated in Ricketts 1994). In this part of the study, obviously altered areas of allanite were avoided, as the goal was to characterize the composition of the allanite prior to alteration. Analytical totals were generally between 98 and 100%, except those of 12A-1 (107.0 wt%) and AP8-1 (95.5%). The microprobe results demonstrate that Ce predominates over Y and all other REE in all allanite grains analyzed, and therefore the mineral corresponds to allanite-(Ce).

In Table 1, iron is presented as FeO<sub>total</sub>. However, both ferric and ferrous iron occur in varying proportions in allanite (Dollase 1971, Deer *et al.* 1986). Therefore, in order to estimate both the ferric and ferrous ion proportions together with the H<sub>2</sub>O content, the following procedure was adopted to recalculate the electron-microprobe results in terms of an empirical formula. First, the atomic proportions were renormalized on the basis of 8 cations assuming no cation vacancies. Then, the molar proportion of OH was calculated by subtracting the renormalized atomic proportions of fluorine and chlorine from unity, assuming that the hydroxyl site is fully occupied by OH, F and Cl. Finally, the proportions of Fe<sup>2+</sup> and Fe<sup>3+</sup> were determined by forcing charge balance between cations and anions. This procedure has the advantage over renormalization to either 13 or 12.5 oxygen atoms (see, for example, Deer *et al.* 1986) of allowing estimates to be made of both ferrous/ferric iron and H<sub>2</sub>O content, but does not result in drastically different results for other constituents of allanite. Peterson & MacFarlane (1993) have reported the pres-

ence of a substitution mechanism involving A-site vacancies according to:  $3Ca^{2+} \leftrightarrow 2REE^{3+} + \square$  in allanite from the Grenville Province of Ontario and Quebec. However, in allanite from the Casto Pluton, most compositions recalculated on the basis of 13 oxygen atoms yield excess cations on all cation sites, which suggests that vacancies are not significant. Thus, we believe that in the case of the Casto Pluton, a recalculation of allanite formulae based on eight cations is valid.

The calculated proportion of ferric iron as a percentage of total iron ranges from 17 to 33%, which is within, but at the lower end of, the range of values reported for allanite previously (Dollase 1971, Deer *et al.* 1986). The resulting H<sub>2</sub>O contents range from 0.93 to 0.96 moles of OH per formula unit, which is also reasonable compared to previously reported values for allanite (Deer *et al.* 1986).

Although the chemical compositions of all allanite grains analyzed in this study are similar, minor compositional variation is noted (Table 1). In general, the magnitude of intragrain variation in composition is comparable to that of the intergrain variation, and both are relatively small. Thus, the allanite grains exhibit no strong zonation, although admittedly the number of points analyzed on each allanite grain is comparatively small. However, a lack of prominent primary zoning is also indicated by X-ray mapping.

A representative empirical formula for the optically most pristine allanite (13A), recalculated as described above, is  $(REE)_{0.83}Ca_{1.07}Th_{0.04}Mn^{2+}_{0.06}(Ti^{4+}_{0.11}Mg^{2+}_{0.04}Fe^{2+}_{0.99}Fe^{3+}_{0.48}Al_{1.38})(Si_{3.00}O_{12})(OH_{0.95}F_{0.05})$ , where REE represents  $(La_{0.14}Ce_{0.41}Pr_{0.05}Nd_{0.17}Sm_{0.03}Y_{0.03})$ . Compared to a variety of allanite samples, the empirical formulas of which are given by Deer *et al.* (1986),

TABLE 1. REPRESENTATIVE COMPOSITIONS OF ALLANITE FROM THE CASTO PLUTON, IDAHO

	12A-1	12A-2	12B-1	12B-2	12B-3	13A-1		13A-2	13B-1	13B-2	13B-3	15A-1	15A-2
SiO <sub>2</sub> , wt.%	30.1	30.4	30.2	30.3	30.2	30.3	SiO <sub>2</sub> , wt.%	30.3	29.8	30.0	30.1	30.3	30.6
TiO <sub>2</sub>	0.94	1.32	1.58	1.71	1.53	1.46	TiO <sub>2</sub>	1.54	2.11	2.31	2.17	2.24	2.45
ThO <sub>2</sub>	0.46	1.86	1.70	1.21	1.12	1.90	ThO <sub>2</sub>	2.12	1.43	0.46	0.50	1.12	0.75
Al <sub>2</sub> O <sub>3</sub>	13.2	12.9	13.1	12.9	12.9	11.8	Al <sub>2</sub> O <sub>3</sub>	12.4	11.9	11.6	11.8	11.6	11.7
Y <sub>2</sub> O <sub>3</sub>	0.29	0.21	0.91	0.16	0.16	0.63	Y <sub>2</sub> O <sub>3</sub>	0.30	0.13	0.11	0.11	0.13	0.12
La <sub>2</sub> O <sub>3</sub>	8.27	5.52	5.51	6.31	6.66	3.96	La <sub>2</sub> O <sub>3</sub>	4.97	6.97	7.87	7.24	7.59	7.59
Ce <sub>2</sub> O <sub>3</sub>	18.1	11.7	11.9	12.5	12.5	11.2	Ce <sub>2</sub> O <sub>3</sub>	11.8	12.7	13.1	13.1	13.2	12.8
Pr <sub>2</sub> O <sub>3</sub>	1.67	1.14	1.20	1.13	1.10	1.35	Pr <sub>2</sub> O <sub>3</sub>	1.23	1.10	1.02	1.10	1.03	1.05
Nd <sub>2</sub> O <sub>3</sub>	5.53	3.96	4.14	3.86	3.49	4.67	Nd <sub>2</sub> O <sub>3</sub>	4.42	3.46	3.23	3.59	3.36	3.43
Sm <sub>2</sub> O <sub>3</sub>	0.59	0.49	0.54	0.41	0.33	0.81	Sm <sub>2</sub> O <sub>3</sub>	0.58	0.35	0.25	0.30	0.27	0.28
MgO	0.26	0.55	0.49	0.69	0.77	0.24	MgO	0.36	0.48	0.75	0.76	0.66	0.75
CaO	8.46	10.3	10.2	10.2	10.0	10.1	CaO	9.87	9.57	9.34	9.64	9.40	9.32
MnO	0.96	0.42	0.28	0.27	0.28	0.72	MnO	0.50	0.38	0.25	0.23	0.35	0.24
FeO	16.5	16.1	16.1	16.2	15.9	17.7	FeO	16.9	16.6	16.2	16.5	16.4	16.6
H <sub>2</sub> O	1.46	1.41	1.40	1.44	1.43	1.40	H <sub>2</sub> O	1.41	1.38	1.37	1.41	1.39	1.40
F	0.14	0.16	0.18	0.14	0.11	0.17	F	0.15	0.19	0.21	0.16	0.19	0.21
Cl	0.02	0.00	0.01	0.00	0.02	0.00	Cl	0.00	0.00	0.02	0.00	0.01	0.00
ΣREE	34.5	23.1	24.2	24.4	24.2	22.7	ΣREE	23.3	24.8	25.3	25.4	25.6	25.3
Total	107.0	98.4	98.4	99.4	98.5	98.2	Total	98.8	98.6	98.1	98.7	99.3	99.2

Electron-microprobe data. Analyses of different spots in the same grain of allanite are distinguished with -1, -2, *etc.*

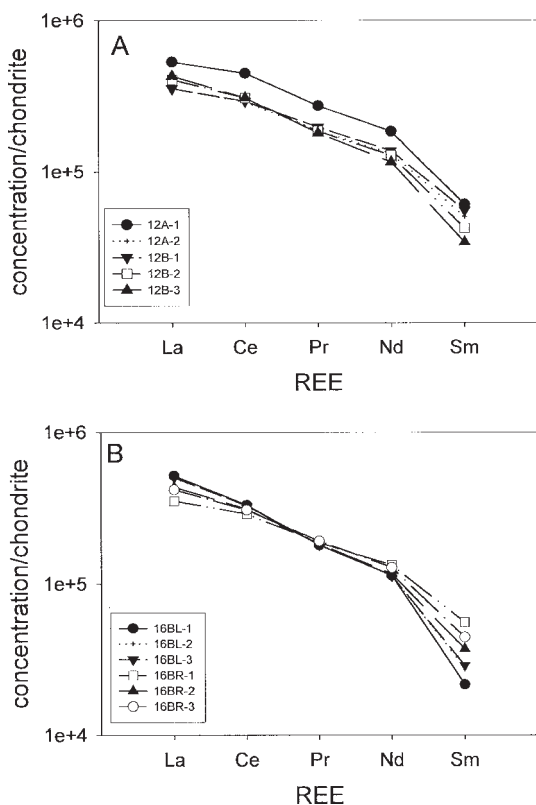


FIG. 2. Plots of chondrite-normalized *REE* concentrations (as determined by electron-microprobe analysis) as a function of *REE* for: A) samples 12A and 12B; B) samples 16B-L and 16B-R. Concentrations of *REE* in chondrite are from Boynton (1984).

allanite-(Ce) in the Casto Pluton has typical Th and total *REE* contents, and its overall composition is not in any way unusual.

The *REE* systematics of allanite-(Ce) from this study are further illustrated in Figure 2, where the *REE* concentrations have been normalized to chondrite concentrations. Most analyses have very similar chondrite-normalized patterns reflecting *LREE*-enrichment, as would be expected for allanite-(Ce), and are concave downward. The chondrite-normalized patterns in Figure 2 also illustrate the lack of significant zoning in most of the allanite grains, as data for different parts of most grains plot very close to one another. The only major exception to this rule is sample 12A, which contains higher levels of the *REE* in the rim than in the center, although the relative proportions of *REE* appear to be constant across the grain. Sample 12A is the most altered allanite grain. The difference in the two points analyzed thus could be a result of removal of components other than the *REE* during alteration, but the

elevated concentrations shown in Figure 2A are suspect because of an analytical total greater than 100% (see Table 1).

Although the degree of compositional variation among allanite grains in the Casto Pluton is comparatively small, systematic variations in composition are detectable and can be related to coupled substitutions. Thorium is accommodated in the allanite structure *via* the coupled substitution:  $\text{Ca}^{2+} + \text{Th}^{4+} \leftrightarrow 2\text{REE}^{3+}$  (Gromet & Silver 1983). A plot of the amount of Ca and Th (in atoms per formula unit, *apfu*) against twice the sum (in *apfu*) of the *REE* and Y in allanite from the Casto pluton is presented in Figure 3A. This plot yields a straight line of negative slope with a correlation coefficient of 0.842. Ideally, the Y intercept of this plot should be 2.0, and the X intercept should be 4.0, *versus* 1.67 and 4.51, respectively, if the coupled substitution in question were the only one taking place. Although the results clearly indicate that the substitution of Th and Ca for two *REE* ions is operative, the deviation of

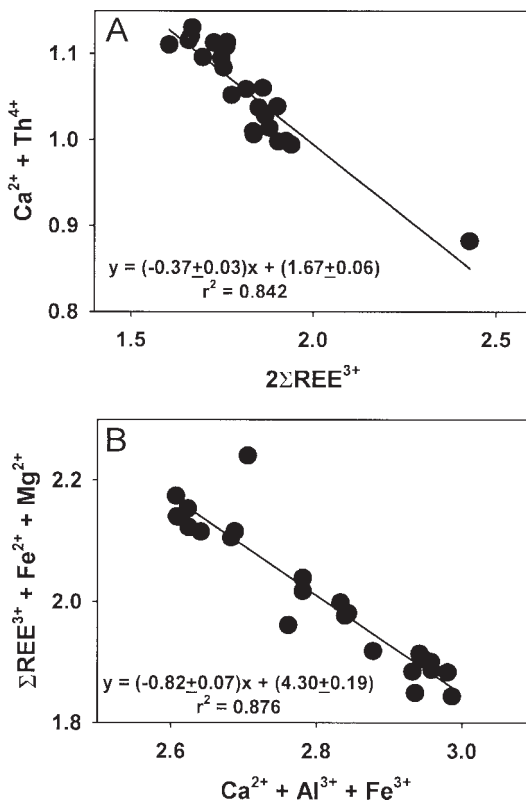


FIG. 3. Plots illustrating potential coupled substitutions in allanite from the Casto pluton. Units are atoms per formula unit (*apfu*). The substitutions plotted are: A)  $\text{Ca}^{2+} + \text{Th}^{4+} \leftrightarrow 2\text{REE}^{3+}$ , B)  $\text{REE}^{3+} + \text{Fe}^{2+} + \text{Mg}^{2+} \leftrightarrow \text{Ca}^{2+} + \text{Al}^{3+} + \text{Fe}^{3+}$ . In all cases, *REE* represents La, Ce, Pr, Nd, Sm, and Y.

the best-fit line from the theoretical one suggests that this is not the only substitution occurring.

According to Deer *et al.* (1986), the fundamental substitution expressing the relationship between epidote and allanite is:  $REE^{3+} + Fe^{2+} \leftrightarrow Ca^{2+} + Fe^{3+}$ . This substitution is generally difficult to test owing to difficulties in determining the relative proportions of ferrous and ferric iron from electron-microprobe results. Another possible substitution related to the latter is:  $REE^{3+} + Fe^{2+} \leftrightarrow Ca^{2+} + Al^{3+}$ , which was tested by plotting  $REE^{3+} + Fe^{2+}$  versus  $Ca^{2+} + Al^{3+}$ . This plot (not shown) yields a straight line with negative slope and a correlation coefficient of 0.718. However, plotting  $REE^{3+} + Fe^{2+} + Mg^{2+}$  versus  $Ca^{2+} + Al^{3+} + Fe^{3+}$  improves the correlation coefficient to 0.876 and lowers the uncertainty of the slope and intercept of the best-fit straight line through the data (Fig. 3B). We therefore suggest that a coupled substitution of the type  $REE^{3+} + Fe^{2+} + Mg^{2+} \leftrightarrow Ca^{2+} + Al^{3+} + Fe^{3+}$  represents much of the observed compositional variation in allanite from the Casto pluton. Moreover, the excellent correlations observed in Figure 3 support the validity of our approach to recalculating the empirical formulas of allanite (the correlations are significantly poorer for empirical formulas based on 13 O). Morin (1977) proposed a rather unusual scheme of coupled substitution:  $REE^{3+} + Ca^{2+} \leftrightarrow Al^{3+} + (Fe^{3+}, Fe^{2+})$  for allanite from granitic rocks in the Kenora – Vermilion Bay area of northwestern Ontario. However, a plot (not shown) of  $REE^{3+} + Ca^{2+}$  versus  $Al^{3+} + (Fe^{3+}, Fe^{2+})$  to test this coupled substitution resulted in a correlation coefficient of close to zero, indicating that this substitution is not important in allanite from the Casto pluton.

#### Characterization of alteration products

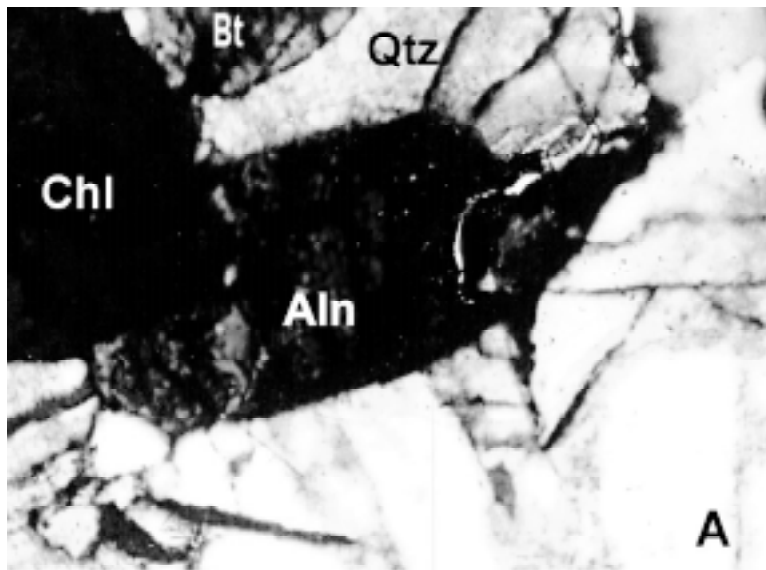
Alteration products of allanite from the Casto pluton were characterized by optical microscopy, back-scattered-electron imaging, X-ray mapping of concentrations of specific elements, and EDS analysis of areas selected based on back-scattered electron (BSE) images and X-ray maps. The findings will be discussed in order of degree of alteration as determined from optical microscopy, from the least to the most altered grain. Photomicrographs, BSE images and X-ray maps of representative grains of allanite studied are presented in Figures 4–6. Images of additional grains are available in Ricketts (1994). In the BSE images, areas with high average atomic number appear dark compared to areas with low average atomic number. In the X-ray maps, concentration of the particular element in question is correlated with brightness, with greater brightness corresponding to higher concentrations.

The least-altered grains of allanite, *i.e.*, 13A, 12B, 15B, AP8 and 13B (not shown), exhibit relatively uniform distributions of the elements considered, suggesting a lack of strong magmatic zoning. However, allanite 13A does display weak zoning, with three zones appar-

ent. The core appears relatively enriched in Ca, La and Ce, and depleted in Th. This core is surrounded by a mantle in which the relative abundances of these elements are reversed, and the mantle in turn is surrounded by a rim relatively enriched in Ca, Ce, and La, and depleted in Th. Because this zonation outlines euhedral sectors of the grain, we consider it to be a primary magmatic feature. In the least-altered grains, phosphorus is either not present in significant amounts or is contained in apatite inclusions. Minor fluorite, identified both optically and by coincident Ca and F anomalies in X-ray maps, is generally present along fractures in, or in the vicinity of, many of these allanite grains.

Allanite grains 16BR (not shown), 15A (Fig. 4) and 16BL (Fig. 5) exhibit moderate degrees of alteration, with depletion of La and Ce, and enrichment of Th along fractures and their outer rim. X-ray maps of allanite grains 16BR (not shown) and 16BL (Fig. 5C) also reveal the presence of substantial P along fractures and rims. Elevated concentrations of F also occur along the rim of allanite 16BR. Whatever the identity of these fracture coatings and rims, their presence is evidently a result of hydrothermal alteration. We suggest that the alteration product around the rim of and within allanite 16BR may be a *REE*–Th phosphate mineral such as monazite, rhabdophane, or brabantite. This interpretation is consistent with the presence of peaks for the light rare-earth elements (*LREE*), Th and P in the EDS scan of a P-rich spot in allanite 16BR. The presence of F in the alteration rim of allanite 16BR remains unexplained, but may be the result of the presence of some fine-grained fluorite admixed with the *REE* phosphate. Qualitative EDS analysis of the Th-rich rim of allanite 15A showed a very large peak for Th, with much smaller peaks for Al, Si, Ca and Fe, suggesting that a portion of the rim has been partially altered to nearly pure Th oxide (thorianite). Coincident patches of high concentrations of Ca and F correspond to fluorite identified optically.

Allanite 12A (Fig. 6) is the most highly altered grain encountered in this study. The X-ray maps for Ca and F (Fig. 6C) reveal several areas where both these elements are strongly concentrated, and in which Si and P are absent. These areas are light purple in plane-polarized light and isotropic under crossed nicols; they are clearly fluorite. It is also notable that the areas containing fluorite are almost devoid of La, Ce, and Th, compared to remnant allanite, but they contain small amounts of Y (Fig. 6C). Qualitative EDS analyses of these areas confirm the presence of Ca and F as the only detectable elements. Fluorite is known to be able to accommodate large quantities of *REE* (up to 14.1 wt.% Ce) and Y (up to 13.7%) according to Clark (1984), but apparently in the Casto pluton, the *LREE* are strongly partitioned into other phases, such as allanite and *REE* phosphate. In a study of the *REE* geochemistry of fluorite from epithermal veins in the general vicinity of the Casto pluton, Constantopoulos (1988) found a range of  $\Sigma REE$



from 2.6 to 130 ppm, consistent with the relatively low *REE* concentrations observed in fluorite in this study.

A characteristic of allanite 12A, aside from the very high degree of alteration and replacement by fluorite, is the occurrence of patches with comparatively high P contents. These patches largely coincide with areas of strong depletion of Si and Ca. Moreover, they contain at least as much La, Ce, and Y as, and possibly more

than, the remnant allanite. Some, but not all, of the P-rich areas are also strongly enriched in Th compared to the remnant allanite. The small rectangular P-rich area at the bottom of the allanite grain, which corresponds to the yellow, birefringent crystal labeled "mnz?" in Figure 6A, is notably enriched in both Y and Th. Thus, the X-ray maps suggest that most of these P-rich patches contain high levels of the *REE*, Y, and Th, in addition to P, and little or no Ca, Si or F. Qualitative EDS analy-

C

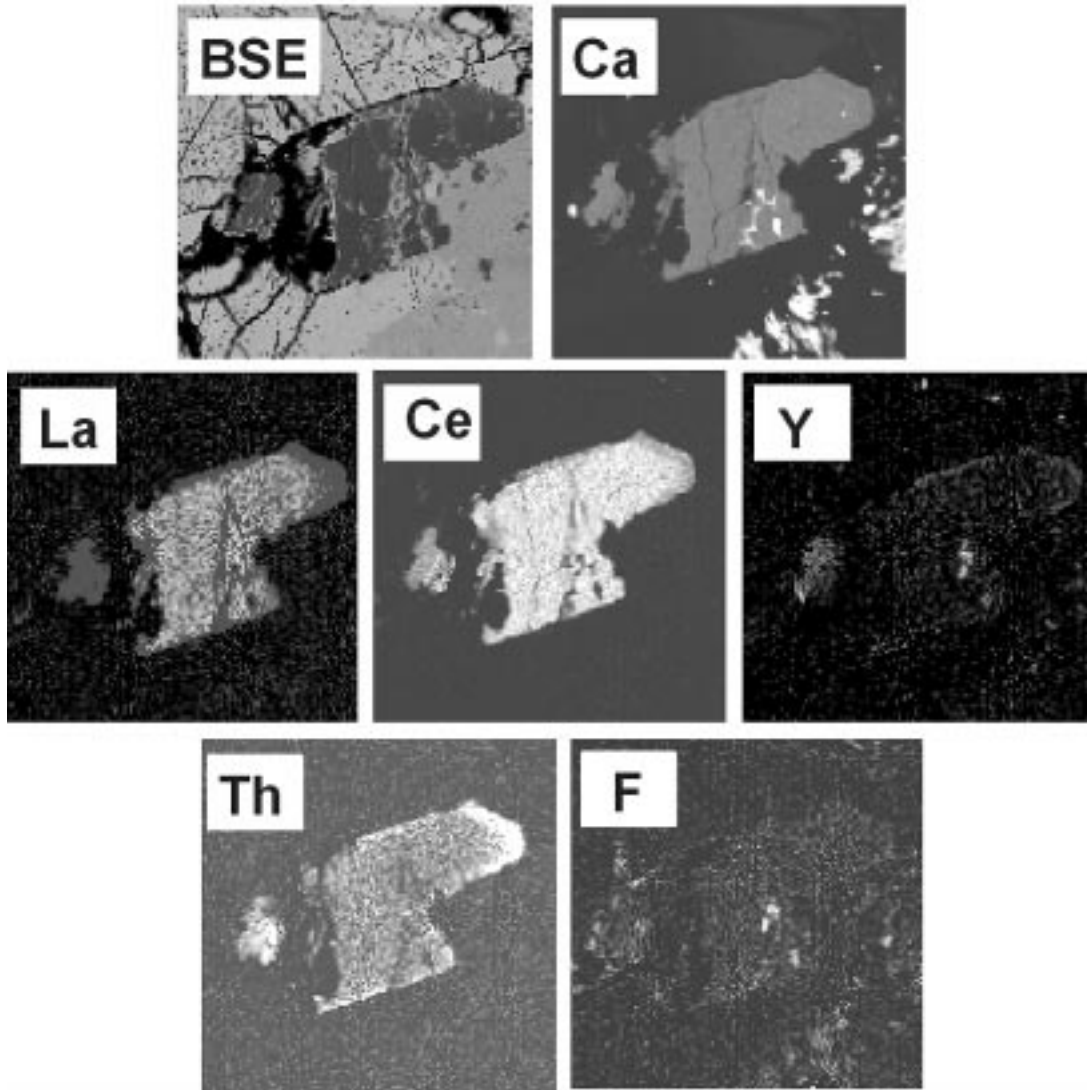
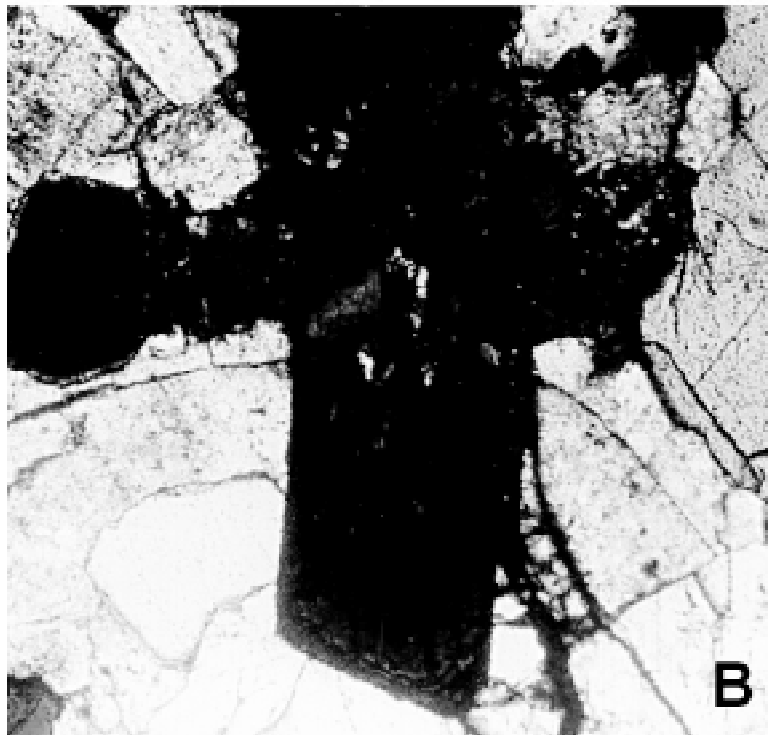
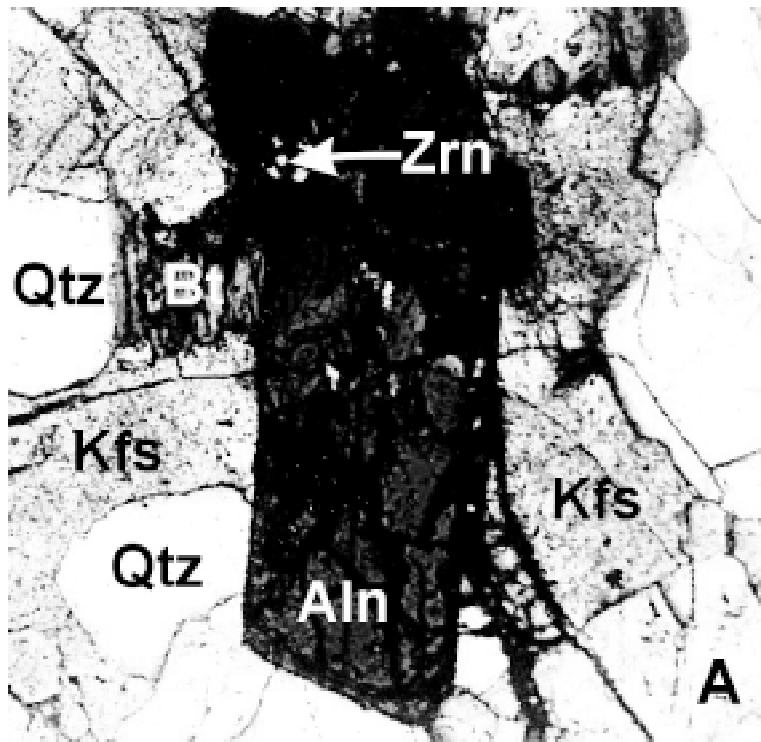


FIG. 4. Photomicrographs of allanite 15A: A) plane-polarized light, B) crossed nicols. The allanite grain is approximately 0.5 mm long. Abbreviations: Aln: allanite, Qtz: quartz, Chl: chlorite, Bt: biotite. C) Back-scattered-electron (BSE) image and X-ray maps of selected elements for allanite 15A. There is a very clear enrichment of Th, and possibly Y, and depletion of La and Ce around the rim of the allanite grain. Some fluorite is visible as elevated Ca and F near the bottom of the allanite grain.

sis of the yellow, birefringent, rectangular grain at the bottom of the allanite grain in Figure 6A confirms that it contains only P, Th, La, Ce (and other *LREE*), with minor Si. This composition is consistent with the replacement of allanite by a *LREE*-Th phosphate, possibly monazite, or the hydrated mineral rhabdophane.

#### *Whole-rock REE concentrations*

The data obtained from neutron-activation analysis of whole-rock samples are shown in Figure 7, which demonstrates a number of points. First, the patterns of all the samples are approximately parallel, small devia-



C

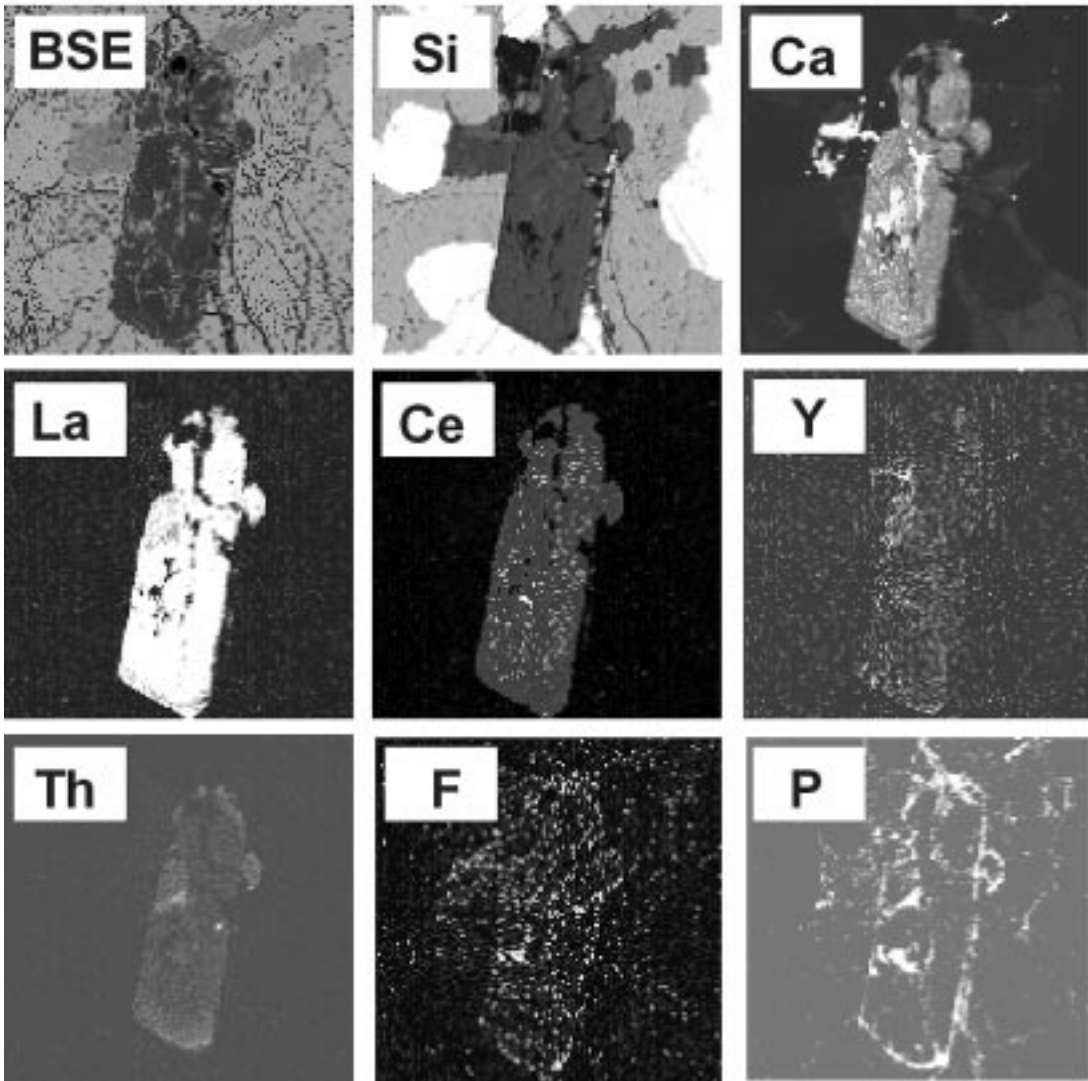
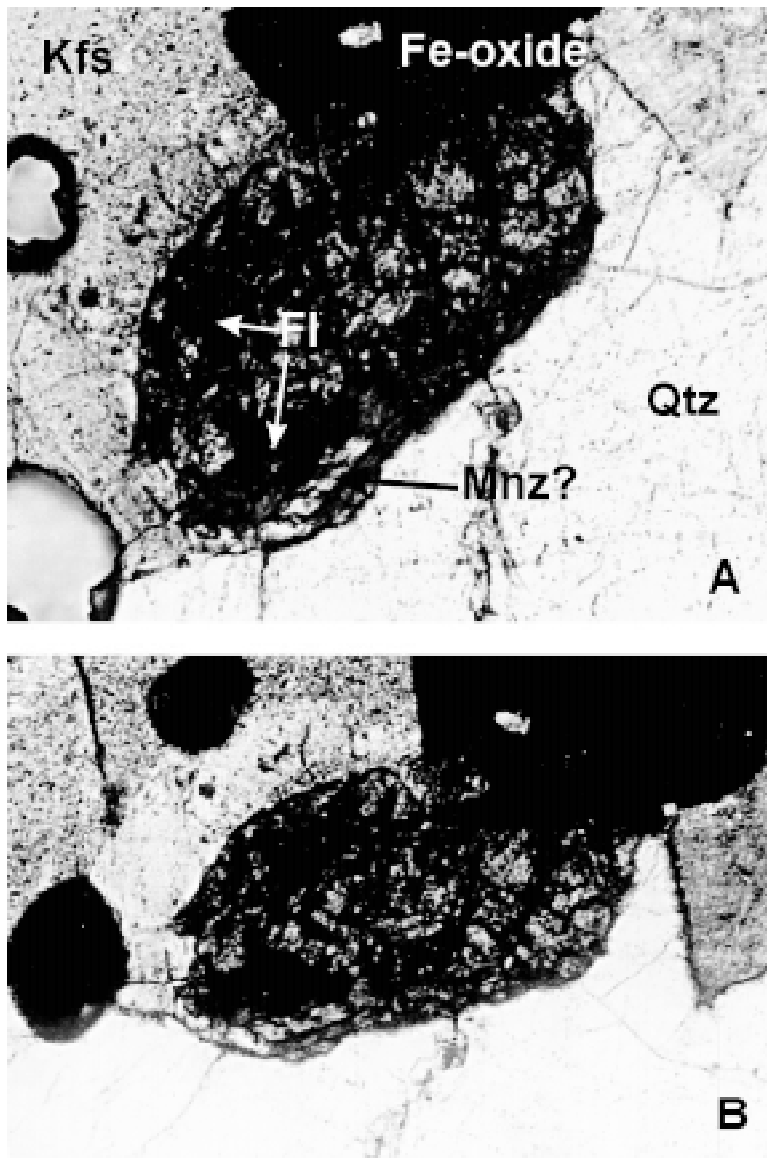


FIG. 5. Photomicrographs of allanite 16BL: A) plane-polarized light, B) crossed nicols. The allanite grain is approximately 0.9 mm long. Abbreviations: Aln: allanite, Qtz: quartz, Bt: biotite, Kfs: K-feldspar, Zrn: zircon. Note the obvious rim or overgrowth along the bottom edge of the allanite grain. C) Back-scattered-electron (BSE) image and X-ray maps of selected elements for allanite 16BL. The rim or overgrowth at the bottom of this allanite grain, so apparent in the photomicrograph, is not obviously different in the BSE image or most of the X-ray maps. However, there is a clear enrichment of P around the entire outer rim of (and along fractures within) the allanite grain.

tions being most likely a consequence of analytical error. Second, the samples are characterized by a general *LREE*-enriched trend, with the *REE* from La to Sm decreasing relatively steeply in chondrite-normalized abundance, and the *REE* from Tb to Lu displaying a relatively flat pattern. Third, all samples exhibit a nega-

tive europium anomaly. Fourth, the *LREE* portion of the patterns for these whole-rock samples is similar to the chondrite-normalized patterns obtained for the allanite grains. Finally, although the rock samples analyzed appear to have been subjected to varying degrees of hydrothermal alteration, there appears to be little relation



between the degree of alteration of allanite and whole-rock *REE* abundances. For example, sample J3, which contains the least-altered grain of allanite, has a pattern very similar to that of sample J2, which contains the most altered grain. In general, hydrothermal alteration appears to have produced no significant fractionation of the *REE* in the whole rock.

#### DISCUSSION

##### *Chemical reactions responsible for alteration of allanite-(Ce)*

Textural evidence clearly suggests that allanite-(Ce) formed during crystallization of the Casto granite and

C

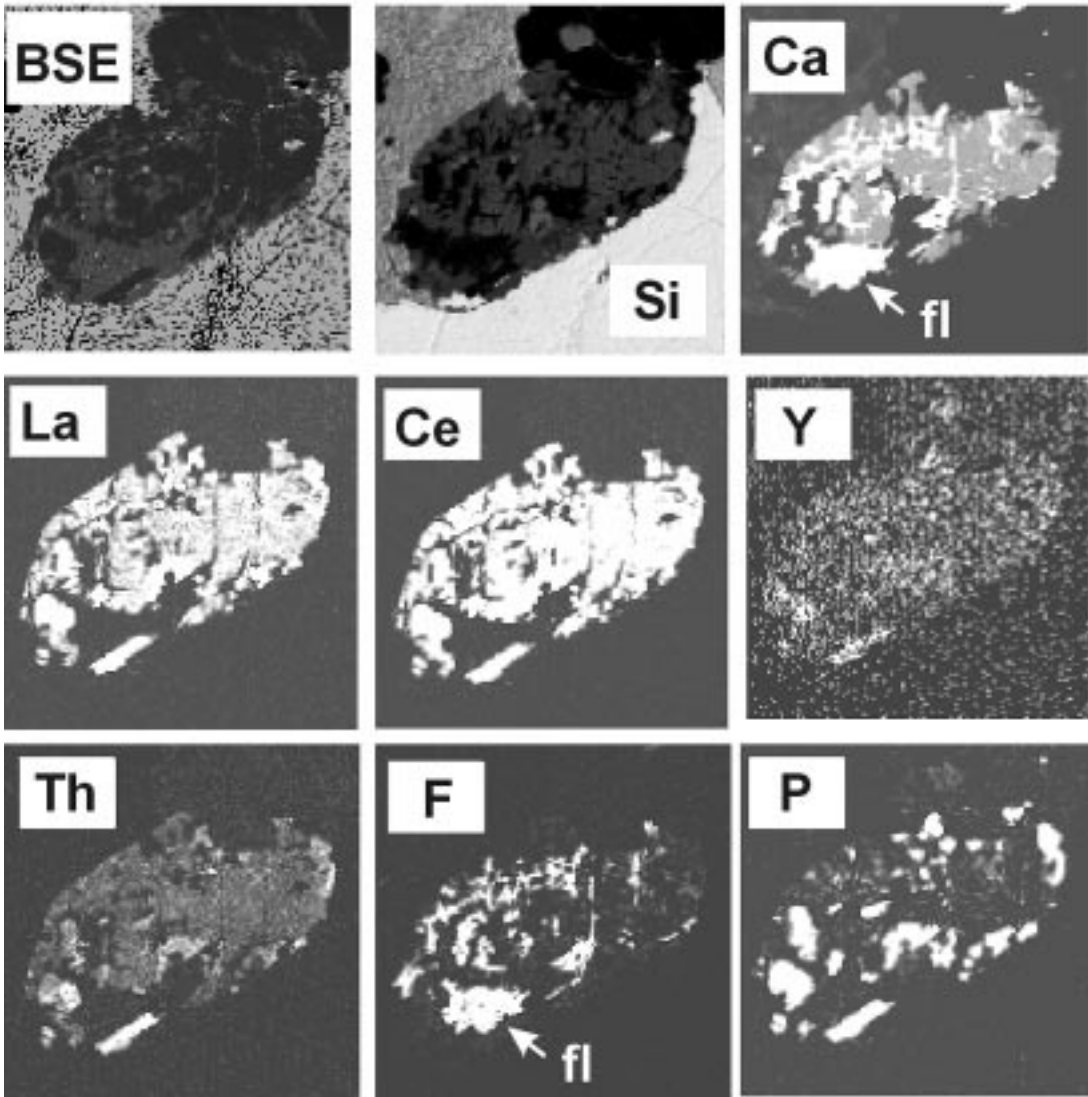


FIG. 6. Photomicrographs of allanite 12A: A) plane-polarized light, B) crossed nicols. The allanite grain is approximately 0.6 mm long. Abbreviations: Aln: allanite, Kfs: K-feldspar, Qtz: quartz, Fl: fluorite, Mnz: monazite. Much of this allanite grain has been altered. C) Back-scattered-electron (BSE) image and X-ray maps of selected elements for allanite 12A. Large areas of this allanite have been replaced by a Ca- and F-rich, REE-, Th- and Si-poor mineral, probably fluorite, and a Th-, REE- and P-rich, Ca-poor mineral, probably monazite.

hence is igneous in origin. However, our results show that at least some allanite grains experienced intense hydrothermal alteration. Allanite-(Ce) that has been altered only slightly exhibits a thin zone of LREE depletion and Th enrichment along fractures and around the rim. Deer *et al.* (1986) indicated that such alteration

“crusts” are commonly observed in allanite. Of more interest here are the products of more intense alteration of allanite, *i.e.*, fluorite and REE-Th phosphate. On the basis of the data we have collected, it is impossible to determine whether the REE-Th-bearing phosphate phase is monazite or rhabdophane. However, in this re-

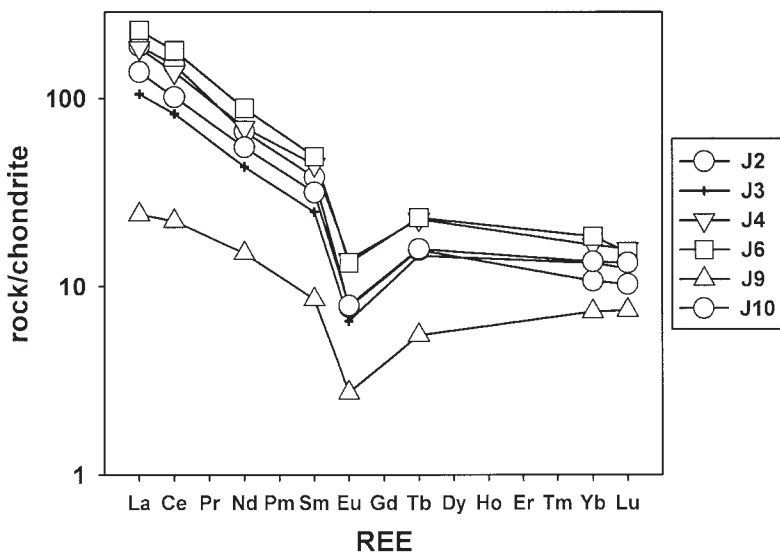
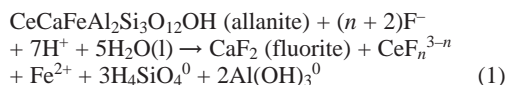


FIG. 7. Chondrite-normalized *REE* data for whole-rock samples from the Casto pluton. Values for chondrite were taken from Boynton (1984). Thin sections containing the allanite grains studied came from some of the same rock samples depicted here, the correspondence being: J2: 12A, J3: 12B, J4: 13A, 13B, J6: 15A, 15B, J9: AP8, J10: 16BL. Note that the patterns are all subparallel and are characterized by *LREE* enrichment and a distinct negative Eu anomaly.

gard, experiments by Akers *et al.* (1993) suggesting that rhabdophane dehydrates to monazite at temperatures at least as low as 200°C (the lowest temperature investigated) are relevant. These authors suggested that rhabdophane is stable only under low-temperature, near-surface conditions, whereas the alteration of allanite-(Ce) most likely took place under hydrothermal conditions. Therefore, for simplicity, we assume the *REE*-Th-bearing phosphate to be monazite-(Ce). This assumption does not affect any of the conclusions we draw.

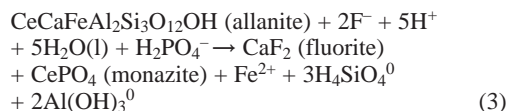
It is likely that the breakdown of allanite and the removal of both *REE* and Th were facilitated by the formation of fluoride complexes of these metals; fluoride is known to form strong complexes with both the *REE* (Wood 1990) and Th (Langmuir & Herman 1980). The breakdown of allanite to monazite and fluorite may have taken place in two steps, although these steps were probably not much separated in time or space. The first step was the dissolution of allanite by a F-rich fluid, with the Ca being fixed by incorporation into fluorite, and the *REE*, Th, Si, Fe, Al and other cations being largely removed from the areas where fluorite forms. A reaction that schematically represents this initial process is:



Although Ce is used in the above equation, similar equations would apply for each of the *REE* and Y. Note that Al and Si could also be complexed by fluoride. The *REE* (and Th) released in the first step, after being transported only on the order of a few tens of micrometers, were then fixed in monazite (and some Th in thorianite) in the second step:



Reaction (2) may have been driven to the right by both an increase in the activity of  $\text{H}_2\text{PO}_4^-$  and a decrease in the activity of  $\text{F}^-$  (*e.g.*, owing to fluorite precipitation). The overall reaction [*i.e.*, the sum of reactions (1) and (2)] may be written:



Some of the dissolved iron may have been subsequently fixed as an iron oxide or hydroxide or chlorite, and some of the Al may have been fixed in white mica, chlorite or a clay mineral.

### Conditions of hydrothermal alteration

We have little direct information on the pressure – temperature – composition conditions of the hydrothermal alteration of allanite-(Ce) in the Casto pluton. However, Constantopoulos (1988) studied fluid inclusions in fluorite from a series of veins in the general vicinity (the Meyers Cove area, see Fig. 1), and his results may provide some insight into the physicochemical conditions prevailing during the alteration of allanite in the Casto pluton, inasmuch as this alteration also clearly involved fluorite-depositing fluids. Constantopoulos (1988) obtained homogenization temperatures ranging from 112° to 238°C, with a mean of 161°C, and with 75% of the data falling within the range 125–185°C. The pressure correction is considered to be <10°C (Constantopoulos 1985). Salinities of the fluids are low, ranging from 0.18 to 1.39 wt.% NaCl eq., with a mean of 0.57 wt.%. Constantopoulos (1988) related the deposition of fluorite in the vicinity of the Casto pluton to the same meteoric hydrothermal system responsible for the zones of low  $\delta^{18}\text{O}$  centered on Eocene plutons in the area (Criss *et al.* 1984). Thus the fluids responsible for regional fluorite mineralization, and by analogy, for the alteration of allanite-(Ce) in the Casto pluton, may be characterized as relatively low-temperature (~160°C), low-salinity (~0.6 wt.% NaCl) meteoric waters that have most likely acquired fluoride from alteration of biotite. The alteration of allanite to a P-rich secondary phase suggests that this fluid also contained phosphate, possibly derived from the dissolution of primary magmatic apatite in the pluton.

### Comparison with previous studies

The replacement of allanite by fluorocarbonates such as bastnäsite and synchysite has been reported in numerous studies (*cf.* Silver & Grunfelder 1957, Sverdrup *et al.* 1959, Adams & Young 1961, Mineyev *et al.* 1962, Ehlmann *et al.* 1964, Mitchell 1966, Riesmeyer 1967, Sakurai *et al.* 1969, Černý & Černa 1972, Pantó 1975, Semenov *et al.* 1978, Mitchell & Redline 1980, Littlejohn 1981, Rimsaite 1982, 1984, Caruso & Simmons 1985, Duda & Nagy 1995). However, there have been fewer reports of the replacement of allanite by phosphate phases during hydrothermal alteration or weathering. Anderson (1960) reported that allanite occasionally appears as remnants in monazite and calcite in Lemhi County, Idaho, suggesting that allanite may have been replaced by the latter phases. Watson & Snyman (1975) described allanite associated with and included in monazite in the Buffalo fluorspar mine, South Africa. Although they did not specifically state that the monazite replaced allanite, the textural descriptions are suggestive of replacement.

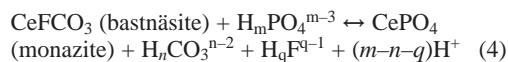
The weathering of allanite to bastnäsite, monazite, clays and iron oxyhydroxides in a granitic pegmatite in Amherst County, Virginia was described by Mitchell &

Redline (1980). Similarly, Meintzer & Mitchell (1988) reported the response of allanite from the Bunker Hill granitic pegmatite in Virginia to intense weathering. They found that allanite was most commonly replaced by monazite and cerianite ( $\text{CeO}_2$ ), although bastnäsite was observed in areas that may have been buffered to higher pH, such as fractures. Thorium was shown to be immobile, but the REE, especially the LREE, were removed during weathering. In our study, we found no evidence of the formation of cerianite, which may be a result of a lower redox potential under the hydrothermal conditions in the Casto pluton compared to the surficial weathering environment of the Bunker Hill pegmatite.

Bingen *et al.* (1996) found allanite to have been replaced by monazite and thorite during the amphibolite-to granulite-facies transition in gneisses from the Rogaland – Vest – Agder sector of Norway. Furthermore, they detected an increase in the medium (MREE) and heavy REE content (HREE) of apatite with increasing grade. They wrote a reaction in which LREE in allanite, and MREE and HREE in hornblende and titanite react with apatite and quartz to produce monazite (LREE) and a lessingite component in apatite (MREE, HREE). This occurrence is relevant to the Casto case in that here apatite also may have served as the source of phosphorus.

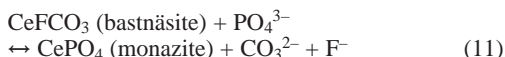
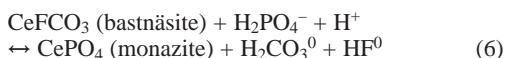
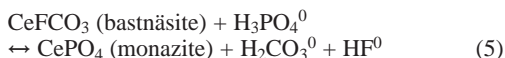
It is interesting to note that the reverse reaction, *i.e.*, the replacement of monazite by allanite, also has been reported to occur (Murata *et al.* 1957, Gable 1980, Ward *et al.* 1992, Broska & Siman 1998, Finger *et al.* 1998). This fact indicates that replacement of allanite by monazite is a reversible process, and as equation (3) would indicate, which phase will be stable is a function of phosphate, calcium, iron, aluminum, silica and hydrogen ion activities. Moreover, allanite of purely hydrothermal origin has been reported from a wide variety of geological environments (Söhnge 1945, Watson & Snyman 1975, Exley 1980, Campbell & Ethier 1984, Gieré 1986, Pan & Fleet 1990, Zakrzewski *et al.* 1992, Kerr & Samson 1998), indicating that the components of allanite can be completely mobilized in aqueous solutions under the appropriate conditions.

In spite of an intensive search, no definitive evidence of fluorocarbonate products of allanite alteration from the Casto pluton was found. The relationship between bastnäsite and monazite can be written in terms of the following generalized reaction:



where  $0 < m < 3$ ,  $0 < n < 2$ , and  $0 < q < 1$ . From reaction (4), it is apparent that the absence of fluorocarbonates could be attributable to a high activity of phosphate or to a low activity or carbonate in the hydrothermal fluid (or both). It is also possible that the actual activity of free  $\text{F}^-$  ion at any given time was maintained at a rela-

tively low value owing to equilibrium constraints with fluorite, even though the total amount of fluoride introduced by the hydrothermal system over its lifetime was significant. The role of pH in determining whether allanite will be altered to bastnäsite or monazite is complicated. Starting at very acidic pH, the following series of reactions applies sequentially as the predominant forms of phosphate, fluoride and carbonate ion change with increasing pH:



The pH values at which the predominant species change are dictated by the dissociation constants of phosphoric, carbonic and hydrofluoric acids, and these constants are temperature- and pressure-dependent. For example, at 25°C and 1 bar, the dominant reactions would change at pH values of 2.1, 4.5, 6.3, 7.0, 10.3 and 12.1. From reactions (5)–(11), it is evident that increased acidity may favor monazite or bastnäsite, or have no effect, depending on the pH range and temperature involved. In any event, none of the possible reactions above has a strong pH dependence in either direction. Thus, it seems unlikely that fluid pH will be as important as the activities of phosphate, carbonate and fluoride in determining whether allanite will alter to bastnäsite or monazite. However, similar reactions written with synchysite, parisite or röntgenite may show stronger pH dependences. Moreover, the activity of  $\text{Ca}^{2+}$  becomes an important variable when considering these Ca-*REE* fluorocarbonates.

#### *Redistribution of REE and Th during alteration of allanite*

The X-ray maps suggest that the *REE* and Th were removed almost completely from areas of allanite replaced by fluorite. However, the areas replaced by the phosphate phase contain very high *REE* and Th con-

tents; it thus appears that, although these elements were remobilized out of allanite locally, they were captured again by the monazite before they were transported any significant distance. More quantitative analytical work would be required before the degree to which the *REE* and Th have been removed can be determined with certainty. Nevertheless, it is clear that in the Casto pluton, the process of leaching of *REE* and Th from allanite was arrested well before it reached completion, in spite of the presence of fluoride.

Although we have not determined quantitatively the degree of mass transfer of *REE* during hydrothermal alteration in the Casto pluton, several considerations suggest that these elements were not mobilized very far. The  $\Sigma\text{REE} + \text{Y}$  contents of allanite in the Casto pluton, determined by electron-microprobe analysis (Table 1), range from 22 to 34 wt.%; in fact, all but one composition fall in the range 23–26 wt.%. We have not quantitatively analyzed the *REE* phosphate that has replaced allanite, but EDS analysis revealed a predominance of *REE*, Th and P. Assuming pure *REE* monazite, the *REE* content would be approximately 59 wt.%. Thus the monazite replacing allanite most likely contains more than twice as much *REE* as the original allanite. The X-ray maps of La, Th and Y (Fig. 6c) are at least consistent with a higher content of these elements in the P-rich sections as compared to the less altered allanite; Ce seems to be more evenly distributed. Klein & Hurlbut (1985) gave a range of densities for allanite, from 3.5 to 4.2 g/cm<sup>3</sup>, and for monazite, from 5.0 to 5.3 g/cm<sup>3</sup>. Thus not only does monazite contain a higher concentration of the *REE* than allanite, but there would also be a modest reduction in volume upon replacement of allanite by monazite. Examination of Figure 6C suggests that, the portions of allanite 12A that were replaced by *REE* phosphate (which contains nearly twice as much *REE* as allanite) are approximately equal in area to the portions replaced by fluorite (from which the *REE* effectively have been removed). Thus the amount of *REE* removed from allanite when it was replaced by fluorite is approximately balanced by the greater quantity of *REE* required to form monazite. These considerations suggest that although the *REE* were locally sufficiently mobile to be removed from allanite, they were fixed in monazite before they were transported over distances greater than a few tens of micrometers.

The one analysis that yielded 34 wt.%  $\Sigma\text{REE} + \text{Y}$  came from allanite 12A, the most altered allanite studied (see also Fig. 6A). Although altered areas were avoided during the microprobe analyses, it is possible that the area yielding this higher  $\Sigma\text{REE} + \text{Y}$  content was partially altered, which may explain the poor analytical total. However, it is interesting that the most altered allanite grain has a higher total *REE* content than most fresh and less altered allanite grains, which is consistent with a lack of large-scale remobilization of the *REE*.

Further evidence for the lack of significant transport of the *REE* by the hydrothermal fluid comes from analy-

sis of the whole-rock granite samples. As pointed out above, the *REE* patterns for all rock samples analyzed are roughly subparallel irrespective of the degree of alteration, as judged on the basis of petrographic criteria; with the exception of sample J9, the abundance patterns exhibit a spread of no more than a factor of 3 or 4. The rock sample containing the most altered allanite studied, J2, has *REE* abundances very similar to those of the sample containing one of the least-altered grains of allanite, J3. Moreover, sample J9, which contains an allanite grain with only a mild degree of alteration, is the only sample with a pattern distinctly displaced from the rest. Even in the latter case, the pattern remains subparallel to all the others. The lack of fractionation of the *REE* as a function of degree of alteration would be unexpected if the *REE* were mobilized over a significant distance by a hydrothermal fluid, because the *LREE* and *HREE* should have significantly different solubilities in a fluoride-bearing hydrothermal fluid. Thus the lack of any systematic relationship of total *REE* abundances with degree of alteration and the fact that the *REE* patterns remain parallel in spite of intense alteration of the allanite strongly suggest that the *REE* were not mobilized over any significant distance. The variable position of the *REE* patterns along the *Y* axis observed in Figure 7 may be a result of variations in the modal abundance of allanite in the original rocks, or the addition or removal of other major, more mobile components of the rock during alteration.

The lack of extensive mobilization of the *REE* upon decomposition of allanite-(Ce) may be attributed to two factors. Firstly, the phosphate activity of the fluid was sufficient to permit the formation of a relatively insoluble *REE*-Th-bearing phosphate, which captured these elements. Secondly, the activity of free fluoride was limited by the solubility of fluorite. Thus, to the extent that the reaction:



proceeds to the right, the activity of free fluoride ion will be decreased, and fluoride complexes of Th and *REE* will become destabilized according to:



and



and these elements may then be more readily removed from solution. At the low temperatures and salinities inferred for the allanite-altering fluids in the Casto pluton, the solubility of fluorite is rather low (Holland & Malinin 1979). Furthermore, the activity of free fluoride would be further lowered by formation of complexes with other components in the hydrothermal fluid, such as  $\text{H}^+$ ,  $\text{Na}^+$ ,  $\text{K}^+$ ,  $\text{Fe}^{2+}$ ,  $\text{Al}^{3+}$ , etc. Thus, a combina-

tion of high phosphate activity and a fluoride activity maintained relatively low by the solubility of fluorite and competitive complexation limited the mobility of the *REE* and Th liberated upon destruction of allanite.

#### *Implications for the disposal of radioactive waste*

The response of allanite to hydrothermal alteration may offer some information on the potential response of deeply buried nuclear waste forms to the incursion of heated groundwaters at some time in the future. Radionuclide-bearing metamict minerals such as allanite represent models for the study of silicate-based waste forms, such as borosilicate glasses, that have been subjected to radiation damage over long time-periods (Ewing 1976). The felsic plutonic and volcanic rocks in the study area are also reasonable analogues of granitic and volcanic rocks under investigation as potential nuclear-waste repositories in many countries. It is expected that deeply buried, high-level radioactive waste and its immediate environment will experience elevated temperatures owing both to the natural geothermal gradient and the excess heat produced by radioactive decay. These temperatures generally are expected to be in the range 150–200°C in a properly designed repository (Brookins 1984, OECD 1984). Thus the hydrothermal fluids responsible for the alteration of allanite in the Casto pluton may have had a temperature similar to that expected for the interaction of heated groundwater with a breached nuclear waste repository.

Although allanite from the Casto pluton contains a lower concentration of radioactive elements than would likely be present in a high-level nuclear waste form, its alteration occurred under the “worst-case” scenario of access by freely circulating hydrothermal fluids containing a strong complexing agent, *i.e.*, fluoride. Even under these adverse conditions, the *REE* and Th released during the hydrothermal alteration of allanite were not transported very far before they were immobilized in secondary phases. We can reasonably expect that this also would be the case for trivalent and tetravalent actinides, for which  $\text{REE}^{3+}$  and  $\text{Th}^{4+}$  are analogues. However, our study does not address the mobility of radionuclides for which the *REE* and Th are not analogues, such as Sr, Cs, or  $\text{U}^{6+}$ , that might be released from nuclear waste. Moreover, there are a number of examples of natural systems in which the *REE* or Th (or both) apparently were transported over relatively great distances. Caution thus is required in extrapolating the results of this study to other environments.

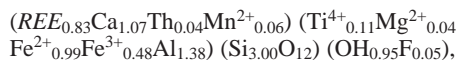
#### CONCLUSIONS

Primary magmatic allanite from the Eocene Casto pluton, Idaho, and the products of its alteration by a fluoride-bearing hydrothermal fluid, were characterized by petrography, electron-microprobe analysis, BSE imaging, X-ray emission mapping and EDS analysis. The

following conclusions have been drawn from this work.

1) Allanite in the Casto pluton exhibits a relatively narrow range in composition, an absence of prominent zoning, and a rather typical composition compared to other occurrences of allanite reported in the literature.

2) A representative empirical formula for the allanite in this study, based on eight cations, is:



where *REE* represents  $(La_{0.14}Ce_{0.41}Pr_{0.05}Nd_{0.17}Sm_{0.03}Y_{0.03})$ .

3) The relatively narrow range of chemical variation observed is consistent with two main coupled substitutions:  $Ca^{2+} + Th^{4+} \leftrightarrow 2REE^{3+}$  and  $REE^{3+} + Fe^{2+} + Mg^{2+} \leftrightarrow Ca^{2+} + Al^{3+} + Fe^{3+}$ .

4) Weak alteration is manifested by a thin zone of slight depletion of *REE* and enrichment in Th around the rim and along fractures of allanite grains. Allanite that has been altered most severely is replaced to a large extent by relatively *REE*- and Th-poor fluorite, a *REE*- and Th-rich phosphate phase, probably monazite, and minor amounts of a Th-only phase, probably thorianite.

5) The overall alteration reaction may be expressed as  $REECaFeAl_2Si_3O_{12}OH_{\text{allanite}} + 2F^- + 5H^+ + 5H_2O(l) + H_2PO_4^- \rightarrow CaF_{2,\text{fluorite}} + REEPO_{4,\text{monazite}} + Fe^{2+} + 3H_4SiO_4^0 + 2Al(OH)_3^0$ , where Fe and Al may ultimately have been fixed in iron oxides, oxyhydroxides, or chlorite, and clays, chlorite or white mica, respectively, or removed from the system.

6) Although locally the *REE* and Th were removed from allanite upon replacement by fluorite, these elements were transported distances of at most a few tens of micrometers before they were fixed in the secondary *REE*-Th phosphate.

7) The alteration described may have been caused by a relatively low-temperature (100–200°C), low-salinity (0–1.4 wt.% NaCl equivalent), fluoride- and phosphate-bearing hydrothermal fluid.

8) The relatively low degree of remobilization of the *REE* and Th in the presence of a fluoride-bearing fluid may be attributable to the ready availability of phosphate and the maintenance of free fluoride activity at relatively low values by competitive complexation with other metals and solubility constraints with respect to fluorite.

9) These results suggest that even if *REE*, Th and analogue actinide elements are released by the interaction of silicate-based waste forms with hydrothermal fluids, they may be immobilized within the repository by the formation of insoluble secondary phases.

#### ACKNOWLEDGEMENTS

We gratefully acknowledge the help and advice given by Dennis Geist and Larry Anovitz, and the receipt of a University of Idaho Seed grant for financial

support of this work. Matt Shawkey and Paul van Middlesworth assisted with the field work. Reviews of the manuscript by Iain Samson, Dennis Geist, Hans-Jürgen Förster, and editor Bob Martin helped clarify our presentation immensely.

#### REFERENCES

- ADAMS, J.W. & YOUNG, E.J. (1961): Accessory bastnäsite in the Pikes Peak granite, Colorado. *U.S. Geol. Surv., Prof. Pap.* **424-C**, 292-294.
- AKERS, W.T., GROVE, M., HARRISON, T.M. & RYERSON, F.J. (1993): The instability of rhabdophane and its unimportance in monazite paragenesis. *Chem. Geol.* **110**, 169-176.
- ANDERSON, A.L. (1960): Genetic aspects of the monazite and columbite-bearing rutile deposits in northern Lemhi County, Idaho. *Econ. Geol.* **55**, 1179-1201.
- BENNETT, E.H. (1980): Granitic rocks of Tertiary age in the Idaho Batholith and their relation to mineralization. *Econ. Geol.* **75**, 278-288.
- \_\_\_\_\_ & KNOWLES, C.R. (1983): Tertiary plutons and related rocks in central Idaho. *U.S. Geol. Surv., Bull.* **1658**, 81-95.
- BINGEN, B., DEMAÏFFE, D. & HERTOGEN, J. (1996): Redistribution of rare earth elements, thorium, and uranium over accessory minerals in the course of amphibolite to granulite facies metamorphism: the role of apatite and monazite in orthogneisses from southwestern Norway. *Geochim. Cosmochim. Acta* **60**, 1341-1354.
- BOATNER, L.A., BEALL, G.W., ABRAHAM, M.M., FINCH, C.B., HURAY, P.G. & RAPPAP, M. (1980): Monazite and other lanthanide orthophosphates as alternate actinide waste forms. In *Scientific Basis for Nuclear Waste Management 2* (C.J.M. Northrup, Jr., ed.). Plenum Press, New York, N.Y.
- BOYNTON, W.V. (1984): Cosmochemistry of the rare earth elements: meteorite studies. In *Rare Earth Element Geochemistry* (P. Henderson, ed.). Elsevier, Amsterdam, The Netherlands (63-114).
- BROOKINS, D.G. (1984): *Geochemical Aspects of Radioactive Waste Disposal*. Springer-Verlag, New York, N.Y.
- BROSKA, I. & SIMAN, P. (1998): The breakdown of monazite in the West-Carpathian Veporic orthogneisses and Tatric granites. *Geol. Carpathica* **49**, 161-167.
- CAMPBELL, F.A. & ETHIER, V.G. (1984): Composition of allanite in the footwall of the Sullivan orebody, British Columbia. *Can. Mineral.* **22**, 507-511.
- CARCANGIU, G., PALOMBA, M. & TAMANINI, M. (1997): *REE-bearing minerals in the albitites of central Sardinia, Italy. Mineral. Mag.* **61**, 271-283.

- CARUSO, L. & SIMMONS, G. (1985): Uranium and microcracks in a 1,000-meter core, Redstone, New Hampshire. *Contrib. Mineral. Petrol.* **90**, 1-17.
- ČERNÝ, P. & ČERNA, I. (1972): Bastnäsite after allanite from Rough Rock Lake, Ontario. *Can. Mineral.* **11**, 541-543.
- CHOPPIN, G.R. (1983): Comparison of the solution chemistry of the actinides and lanthanides. *J. Less-Common Metals* **93**, 323-330.
- \_\_\_\_\_ (1986): Speciation of the trivalent *f*-elements in natural waters. *J. Less-Common Metals* **126**, 307-313.
- \_\_\_\_\_ (1989): Soluble rare earth and actinide species in seawater. *Mar. Chem.* **28**, 19-26.
- CLARK, A.M. (1984): Mineralogy of the rare earth elements. In *Rare Earth Element Geochemistry* (P. Henderson, ed.). Elsevier, Amsterdam, The Netherlands (33-61).
- CONSTANTOPOULOS, J. (1985): *Fluid Inclusions and Geochemistry of Fluorite from the Challis 1° × 2° Quadrangle, Idaho*. M.S. thesis, Univ. of Idaho, Moscow, Idaho.
- \_\_\_\_\_ (1988): Fluid inclusions and rare earth element geochemistry of fluorite from south-central Idaho. *Econ. Geol.* **83**, 626-636.
- CRISS, R.E., EKREN, E.B. & HARDYMAN, R.F. (1984): Casto ring zone: a 4,500 km<sup>2</sup> fossil hydrothermal system in the Challis volcanic field, central Idaho. *Geology* **12**, 31-334.
- DEER, W.A., HOWIE, R.A. & ZUSSMAN, J. (1986): *Rock-Forming Minerals. 1B. Disilicates and Ring Silicates* (2nd ed.). John Wiley & Sons, New York, N.Y.
- DOLLASE, W.A. (1971): Refinement of the crystal structure of epidote, allanite, and hancockite. *Am. Mineral.* **56**, 447-463.
- DRAKE, M.J. & WEILL, D.F. (1972): New rare-earth element standards for electron microprobe analysis. *Chem. Geol.* **10**, 179-181.
- DUDA, G. & NAGY, G. (1995): Some REE-bearing accessory minerals in 2 types of Variscan granitoids, Hungary. *Geol. Carpathica* **46**, 67-78.
- EHLMANN, A.J., WALPER, J.L. & WILLIAMS, J. (1964): A new, Barringer Hill-type, rare-earth pegmatite from the Central Mineral Region, Texas. *Econ. Geol.* **59**, 1348-1360.
- EWING, R.C. (1976): Metamict mineral alteration: an implication for radioactive waste disposal. *Nature* **192**, 1336-1337.
- EXLEY, R.A. (1980): Microprobe studies of REE-rich accessory minerals: implications for Skye granite paragenesis and REE mobility in hydrothermal systems. *Earth Planet. Sci. Lett.* **48**, 97-110.
- FINGER, F., BROSKA, I., ROBERTS, M.P. & SCHERMAIER, A. (1998): Replacement of primary monazite by apatite – allanite – epidote coronas in an amphibolite facies granite gneiss from the Eastern Alps. *Am. Mineral.* **83**, 248-258.
- FISHER, F.S. & JOHNSON, K.M. (1995): Geology and mineral resource assessment of the Challis 1° × 2° quadrangle, Idaho. *U.S. Geol. Surv., Prof. Pap.* **1525**.
- \_\_\_\_\_, MCINTYRE, D.H. & JOHNSON, K.M. (1992): Geologic map of the Challis 1° × 2° quadrangle, Idaho. *U.S. Geol. Surv., Misc. Invest. Ser., Map I-1819*.
- GABLE, D.J. (1980): The Boulder Creek Batholith, Front Range, Colorado. *U.S. Geol. Surv., Prof. Pap.* **1101**.
- GIERÉ, R. (1986): Zirconolite, allanite and hoegbomite in a marble skarn from the Bergell contact aureole: implications for mobility of Ti, Zr and REE. *Contrib. Mineral. Petrol.* **93**, 459-470.
- GROMET, L.P. & SILVER, L.T. (1983): Rare earth element distributions among minerals in a granodiorite and their petrogenetic implications. *Geochim. Cosmochim. Acta* **47**, 925-939.
- HOLLAND, H.D. & MALININ, S.D. (1979): The solubility and occurrence of non-ore minerals. In *Geochemistry of Hydrothermal Ore Deposits* (H.L. Barnes, ed.; second edition). John Wiley & Sons, New York, N.Y. (461-508).
- KERR, I.D. & SAMSON, I.M. (1998): REE mineralogy of the Pea Ridge Fe-REE deposit, Missouri. *Geol. Soc. Am., Abstr. Programs* **30**, A-370.
- KLEIN, C. & HURLBUT, C.S., JR. (1985): *Manual of Mineralogy* (20<sup>th</sup> ed.). John Wiley & Sons, New York, N.Y.
- LANGMUIR, D. & HERMAN, J.S. (1980): The mobility of thorium in natural waters at low temperatures. *Geochim. Cosmochim. Acta* **44**, 1753-1766.
- LARSON, P. & GEIST, D. (1995): On the origin of low δ<sup>18</sup>O magmas: evidence from the Casto pluton, Idaho. *Geology* **23**, 909-912.
- LEWIS, R.S. & KILSGAARD, T.H. (1991): Eocene plutonic rocks in south central Idaho. *J. Geophys. Res.* **96**, 295-311.
- LITTLEJOHN, A.L. (1981): Alteration products of accessory allanite in radioactive granites from the Canadian Shield. *Curr. Res., Geol. Surv. Can., Pap.* **81-1B**, 95-104.
- MCINTYRE, D.H., EKREN, E.B. & HARDYMAN, R.F. (1982): Stratigraphic and structural framework of the Challis Volcanics in the eastern half of the Challis 1° × 2° quadrangle, Idaho. In *Cenozoic Geology of Idaho* (B. Bonnicksen & R.M. Beckenridge, eds.). *Idaho Bureau of Mines and Geology, Bull.* **26**, 3-22.
- MEINTZER, R.E. & MITCHELL, R.S. (1988): The epigene alteration of allanite. *Can. Mineral.* **26**, 945-955.
- MILLERO, F.J. (1992): Stability constants for the formation of rare earth inorganic complexes as a function of ionic strength. *Geochim. Cosmochim. Acta* **56**, 3123-3132.
- MINEYEV, D.A., MAKAROKHIN, B.A. & ZHABIN, A.G. (1962): On the behavior of the lanthanides during alteration of rare earth minerals. *Geochemistry* **2**, 684-693.

- MITCHELL, R.S. (1966): Virginia metamict minerals: allanite. *Southeast. Geol.* **7**, 183-195.
- \_\_\_\_\_ & REDLINE, G.E. (1980): Minerals of a weathered allanite pegmatite, Amherst County, Virginia. *Rocks & Minerals* **55**, 245-249.
- MORIN, J.A. (1977): Allanite in granitic rocks of the Kenora – Vermilion Bay area, northwestern Ontario. *Can. Mineral.* **15**, 297-302.
- MURATA, K.J., ROSE, H.J., JR., CARRON, M.K. & GLASS, J.J. (1957): Systematic variation of rare-earth elements in cerium-earth minerals. *Geochim. Cosmochim. Acta* **11**, 141-161.
- OECD (1984): Geological disposal of radioactive waste. An overview of the current status of understanding and development. Report Sponsored by the Comm. Eur. Commun. and the OECD Nucl. Energy Agency. Published by the Org. Econ. Co-op. & Dev., Paris, France.
- PAN, YUANMING & FLEET, M.E. (1990): Halogen-bearing allanite from the White River gold occurrence, Hemlo area, Ontario. *Can. Mineral.* **28**, 67-75.
- PANTÓ, G. (1975): Trace minerals and the granitic rocks of the Valence and Necsok Mountains. *Acta Geol. Acad. Sci., Hungary* **19**, 59-93.
- PETERSON, R.C. & MACFARLANE, D.B. (1993): The rare-earth-element chemistry of allanite from the Grenville Province. *Can. Mineral.* **31**, 159-166.
- ROEDER, P.L. (1985): Electron-microprobe analysis of minerals for REE: use of calculated peak-overlap corrections. *Can. Mineral.* **23**, 263-271.
- RICKETTS, A. (1994): *The Alteration of Allanites in the Casto Granite Pluton, Central Idaho*. M.S. thesis, Univ. of Idaho, Moscow, Idaho.
- RIESMEYER, W.D. (1967): Bastnäsite after allanite in the Rutherford pegmatite, Amelia County, Virginia. *Virg. J. Sci.* **18**, 188 (abstr.).
- RIMSAITE, J. (1982): The leaching of radionuclides and other ions during alteration and replacement of accessory minerals in radioactive rocks. *Geol. Surv. Can., Pap.* **81-1B**, 253-266.
- \_\_\_\_\_ (1984): Selected mineral associations in radioactive and REE occurrences in the Baie-Johan-Beetz area, Quebec: a progress report. *Geol. Surv. Can., Pap.* **84-1A**, 129-145.
- SÆBØ, P.C. (1961): Contributions to the mineralogy of Norway. No. 11. On lanthanite in Norway. *Norsk Geol. Tidsskr.* **41**, 311-317.
- SAKURAI, K., WAKITA, H., KATO, A. & NAGASHIMA, K. (1969): Chemical studies of minerals containing rarer elements from the Far East. LXIII. Bastnäsite from Karasugawa, Fukushima Prefecture, Japan. *Bull. Chem. Soc. Japan* **42**, 2725-2728.
- SEMENOV, E.I., UPENDRAN, R. & SUBRAMANIAN, V. (1978): Rare earth minerals of carbonatites of Tamil Nadu. *J. Geol. Soc. India* **19**, 550-557.
- SILVER, L.T. & GRUNENFELDER, M. (1957): Alteration of accessory allanite in granites of the Elberton area, Georgia. *Geol. Soc. Am., Bull.* **68**, 1796 (abstr.).
- SÖHNGE, P.G. (1945): The structure, ore genesis and mineral sequence of the cassiterite deposits of the Zaaiploats tin mine, Potgietersrus district, Transvaal. *Trans. Geol. Soc. S. Afr.* **47**, 157-181.
- STRECKEISEN, A.L. (1973): Plutonic rocks – classification and nomenclature recommended by the IUGS subcommission on the systematics of igneous rocks. *Geotimes* **18**, 26-30.
- SVERDRUP, T.L., BRYN, K.O. & SÆBØ, P.C. (1959): Contributions to the mineralogy of Norway. No. 2. Bastnäsite, a new mineral for Norway. *Norsk Geol. Tidsskr.* **39**, 237-247.
- VAN MIDDLESWORTH, P.E. & WOOD, S.A. (1998): The aqueous geochemistry of the rare earth elements and yttrium. 7. REE, Th and U contents in thermal springs associated with the Idaho Batholith. *Appl. Geochem.* **13**, 861-884.
- WARD, C.D., MCARTHUR, J.M. & WALSH, J.N. (1992): Rare earth element behaviour during evolution and alteration of the Dartmoor granite, SW England. *J. Petrol.* **33**, 785-815.
- WATSON, M.D. & SNYMAN, C.P. (1975): The geology and the mineralogy of the fluorite deposits at the Buffalo fluorspar mine on Buffelsfontein, 347KR, Naboomspruit district. *Trans. Geol. Soc. S. Afr.* **78**, 137-151.
- WOOD, S.A. (1990): The aqueous geochemistry of the rare earth elements and yttrium. 2. Theoretical predictions of speciation in hydrothermal solutions to 350°C at saturated water pressure. *Chem. Geol.* **88**, 99-125.
- ZAKRZEWSKI, M.A., LUSTENHOUWER, W.J., NUGTEREN, H.J. & WILLIAMS, C.T. (1992): Rare-earth minerals yttrian zirconolite and allanite-(Ce) and associated minerals from Koberg mine, Bergslagen, Sweden. *Mineral. Mag.* **56**, 27-35.

Received June 3, 1999, revised manuscript accepted February 22, 2000.